

Z' -boson dilepton searches and the high- x quark density

J. Fiaschi,^{1,*} F. Giuli,^{2,†} F. Hautmann,^{2,3,4,‡} S. Moch,^{5,§} and S. Moretti^{6,7,¶}

¹*Department of Mathematical Sciences, University of Liverpool, Liverpool L69 3BX*

²*CERN, European Organization for Nuclear Research, 1 Esplanade des Particules, 1211 Meyrin*

³*Elementaire Deeltjes Fysica, Universiteit Antwerpen, B 2020 Antwerpen*

⁴*Theoretical Physics Department, University of Oxford, Oxford OX1 3PU*

⁵*II. Institut für Theoretische Physik, Universität Hamburg, Luruper Chaussee 149, 22761 Hamburg*

⁶*School of Physics and Astronomy, University of Southampton, Highfield, Southampton SO17 1BJ*

⁷*Department of Physics and Astronomy, Uppsala University, Box 516, SE-751 20 Uppsala*

We study the influence of theoretical systematic uncertainties due to the quark density on LHC experimental searches for Z' -bosons. Using an approach originally proposed in the context of the ABMP16 PDF set for the high- x behaviour of the quark density, we presents results on observables commonly used to study Z' signals in dilepton channels.

Introduction. Beyond-the-Standard-Model (BSM) searches for heavy neutral spin-1 Z' -bosons [1] are carried out at the Large Hadron Collider (LHC) [2, 3] by the ATLAS [4] and CMS [5] collaborations and will continue at the High-Luminosity LHC (HL-LHC) [6, 7] and future colliders [8]. For narrow Z' states, experimental analyses rely on resonant mass searches. For BSM scenarios involving Z' states with large width, the collider sensitivity to new physics signals is influenced significantly by the theoretical modelling of both signal and background [9]. In this case, one of the main sources of systematic uncertainties, affecting the potential of experimental searches for discovering or setting exclusion bounds on new Z' bosons, is given by the Parton Density Functions (PDFs), describing the Quantum Chromo-Dynamics (QCD) evolution of the initial partonic states entering the collision.

The crucial role of the PDFs can be illustrated, e.g., by the analysis [10] of Drell-Yan (DY) processes, i.e., dilepton channels in hadronic collisions. This paper examines broad vector resonances in BSM strongly-interacting Higgs models [11, 12], using the 4-Dimensional Composite Higgs Model (4DCHM) realisation [13] of the minimal composite Higgs scenario [14]. The PDF systematic uncertainties are dominated by the quark sector, for moderate to large momentum fractions x . It is shown in Ref. [15], by an **xFitter** [16, 17] “profiling” analysis, that the quark PDF systematics in this region can be improved by exploiting, besides unpolarised DY production, the experimental information on the SM vector boson polarisation in the DY mass range near the SM vector boson peak. More precisely, “improved PDFs” [15] are obtained by combining high-statistics precision measurements of DY lepton-charge and forward-backward [18–21] asymmetries, associated with the difference between the left-handed and right-handed vector boson polarisation fractions. Ref. [10] demonstrates that the LHC sensitivity to the BSM large-width states is then greatly in-

creased compared to the case of base PDF sets.

The purpose of this note is to investigate further aspects of the PDF systematics in the Z' -boson dilepton search region, concentrating on the effect, pointed out in Ref. [22], of the $x \rightarrow 1$ behaviour of the quark densities. The very high mass tails of physical distributions are influenced by the quark density at high x and low mass scales through QCD evolution, in particular through a combination of non-diagonal contributions to the flavour-singlet evolution kernel [22]. This sensitivity can be recast as a parameterisation uncertainty $(1 - x)^b$ in the nearly-vanishing quark density as $x \rightarrow 1$ [23]. We will follow the approach proposed in [22] to treat the $x \rightarrow 1$ quark density and analyse its impact on the multi-TeV mass region relevant for BSM Z' searches.

We remark that this approach can be regarded as a method to take into account certain kinds of theoretical uncertainties, associated with PDF determinations, which go beyond the standard uncertainties provided by the main PDF sets. Full approaches to producing PDF sets with theory uncertainties are currently being investigated by several groups, e.g., see [24, 25] and ongoing **xFitter** [17] studies based on the method of [26, 27]. For the problem of interest in this paper we use the simple approach of [22], as a complete study will only become possible once PDF sets with full theory uncertainties are available.

We proceed in the following manner. We start by describing the criteria to construct the PDF ensemble through which we parameterise systematic uncertainties in the quark density at high x . Then we consider dilepton observables which are commonly used for BSM searches in the multi-TeV region, the dilepton invariant mass spectrum of the differential cross section, $d\sigma/dM_{\ell\ell}$, and reconstructed forward-backward asymmetry A_{FB}^* . The reconstruction follows the standard prescription based on the boost of the dilepton system, as described in Ref. [28].

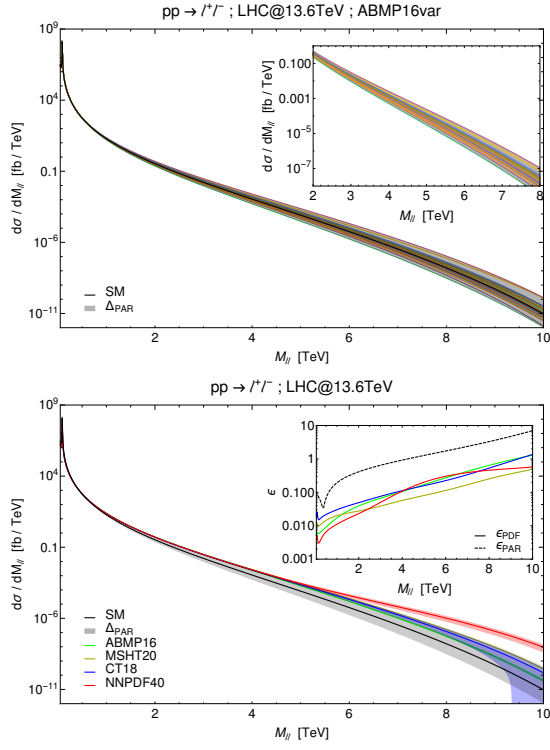


FIG. 1. Differential cross section in invariant mass of the dilepton final state at the LHC with $\sqrt{s} = 13.6$ TeV: (top) results for all ABMP16var members, with the inset plot focusing on the few TeV invariant mass region; (bottom) ABMP16var result compared with results from standard PDF sets, with the inset plot showing the relative sizes of parameterisation and “standard” PDF uncertainties.

We study these observables in two stages.

First, we compute $d\sigma/dM_{\ell\ell}$ and A_{FB}^* in the SM by including the high- x quark density systematics. We compare these results both with those based on the original ABMP16 set [22] from which the PDF ensemble to study the high- x systematics is derived and with those from other commonly used PDF sets, CT18 [29], MSHT20 [30] and NNPDF4.0 [31]. This provides us with a validation test and a quantitative estimate of the impact of high- x systematics on SM predictions. An investigation of the asymmetry A_{FB}^* in the SM has been recently carried out in [32]. Further studies on the A_{FB}^* in the context of PDF determinations may be found in [33–41].

Second, we consider BSM benchmark models for heavy Z' bosons representative of the E_6 , Generalised Left-Right (GLR) and Generalised Standard Model (GSM) [3]. We study the signal profiles in the invariant mass spectrum of the cross section and A_{FB}^* , by discussing them in the light of the high- x quark density systematics.

Quark density at large x . To study the impact of high- x quark densities on dilepton observables, we construct a PDF ensemble as follows. The “central” value of the

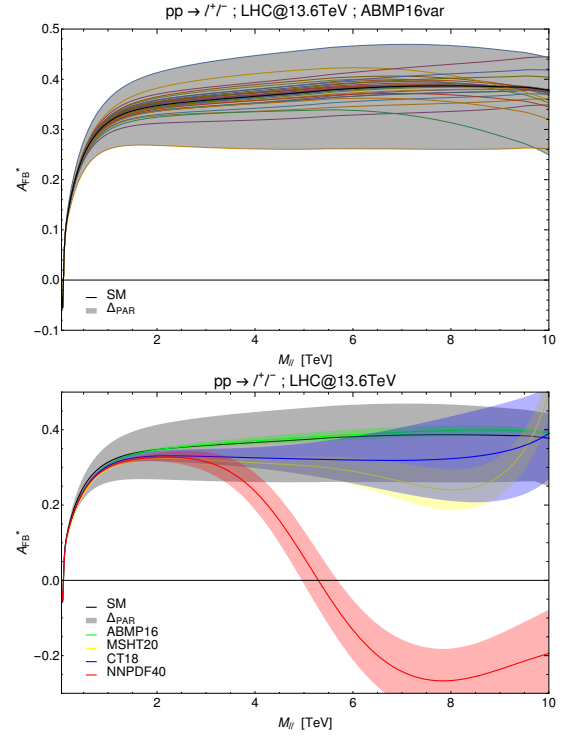


FIG. 2. Asymmetry A_{FB}^* in invariant mass of the dilepton final state at the LHC with $\sqrt{s} = 13.6$ TeV: (top) results for all ABMP16var members; (bottom) ABMP16var result compared with results from standard PDF sets.

ensemble is obtained using the results of the fit contained in Tab.VII of Ref. [22]. We then construct 24 ensemble members by varying the exponent of the $(1-x)$ term of the parameterisation of u and d quarks and antiquarks by $\pm 0.3, 0.5, 1.0$. We obtain predictions for dilepton observables using 22 members of the set, excluding the members with variations by $+1$ for u and by -1 for d as these do not yield a sufficiently fast fall-off in the ratio d/u for $x \rightarrow 1$. We further include predictions obtained from the following additional members.

1. All quark and antiquark distributions varied simultaneously by $\pm 0.3, 0.5, 1$ (i.e., 6 additional variations). We name this Variation #1.
2. Quark distributions varied by ± 1 and antiquark distributions varied by ∓ 1 simultaneously (i.e., 2 additional variations). We name this Variation #2.

All these combinations ensure a vanishing d/u ratio as $x \rightarrow 1$. In the following the predictions obtained from the PDF ensemble described above will be referred to as “ABMP16var”, and the envelope from the 30 different variations will be used as an estimate of the parameterisation uncertainty. We will investigate the impact of this additional uncertainty on observables of the dilepton final state.

SM results. Using the above method ABMP16var, we now compute the dilepton invariant mass distribution

of the differential cross section $d\sigma/dM_{\ell\ell}$ and forward-backward asymmetry A_{FB}^* in the SM. The results are given in Fig. 1 for $d\sigma/dM_{\ell\ell}$ and in Fig. 2 for A_{FB}^* .

The top panels of these figures show the results for all the variations in the ABMP16var ensemble, and the parameterisation uncertainty Δ_{PAR} from their envelope. For $d\sigma/dM_{\ell\ell}$ the largest variations are obtained from Variation #1, while for A_{FB}^* the largest variations are obtained from Variation #2. The inset plot of the top panel in Fig. 1 focuses on the few TeV invariant mass region, relevant for BSM searches at the LHC.

In the bottom panels of Figs. 1 and 2, the ABMP16var results are compared with the results from the original ABMP16 set [22] and other commonly used sets CT18 [29], MSHT20 [30] and NNPDF4.0 [31]. The parameterisation uncertainty Δ_{PAR} is compared with the “standard” PDF uncertainties for each set. The bottom panel of Fig. 1 indicates that the predictions for the SM differential cross section agree for all PDF sets within uncertainties, except NNPDF4.0 which departs from the others for $M_{\ell\ell} \gtrsim 5$ TeV. The inset plot of the bottom panel in Fig. 1 displays the relative sizes $\epsilon = \Delta\sigma/\sigma$ of the parameterisation uncertainties (ϵ_{PAR}) and PDF uncertainties of each set (ϵ_{PDF}), illustrating that the former is roughly one order of magnitude larger than the latter.

The bottom panel of Fig. 2 gives the SM predictions for the forward-backward asymmetry A_{FB}^* from different PDF sets. It shows that the NNPDF4.0 [31] set leads to results for the A_{FB}^* which are similar to those of the ABMP16 [22], CT18 [29] and MSHT20 [30] sets for $M_{\ell\ell} \lesssim 4$ TeV but, for $M_{\ell\ell} \gtrsim 4$ TeV, start to differ dramatically from those of the other sets, which remain similar, within PDF uncertainties, among each other. The NNPDF prediction acquires a negative slope, decreases toward zero and becomes negative above $M_{\ell\ell} \approx 5$ TeV, while the predictions from the other sets stay positive, and roughly flat. The NNPDF behaviour has been discussed at length in the recent work of Ref. [32]. Here we limit ourselves to making a few general remarks, particularly in the light of the method of the present paper to study the high- x quark density systematics.

The peculiar NNPDF prediction for A_{FB}^* at large masses in the SM stems from the fact that the NNPDF4.0 [31] set has antiquark distributions falling much more slowly at high x than all the other sets and, conversely, quark distributions falling much faster at high x than the other sets [32]. This “high-sea, low-valence” scenario applies to all light flavours, and is especially pronounced for the \bar{u} and d distributions. In general, for A_{FB}^* to stay positive one has to have the slope of the antiquark’s fall-off to be larger than the slope of the quark’s fall-off for all values of x . This condition is fulfilled by the PDF sets [22, 29, 30], but it is not fulfilled by the NNPDF set [31], starting approximately for $x \gtrsim 0.4$ [32]. This feature of the NNPDF sea and valence quark distributions, particularly in the region $0.4 \lesssim x \lesssim 0.6$, is responsible for

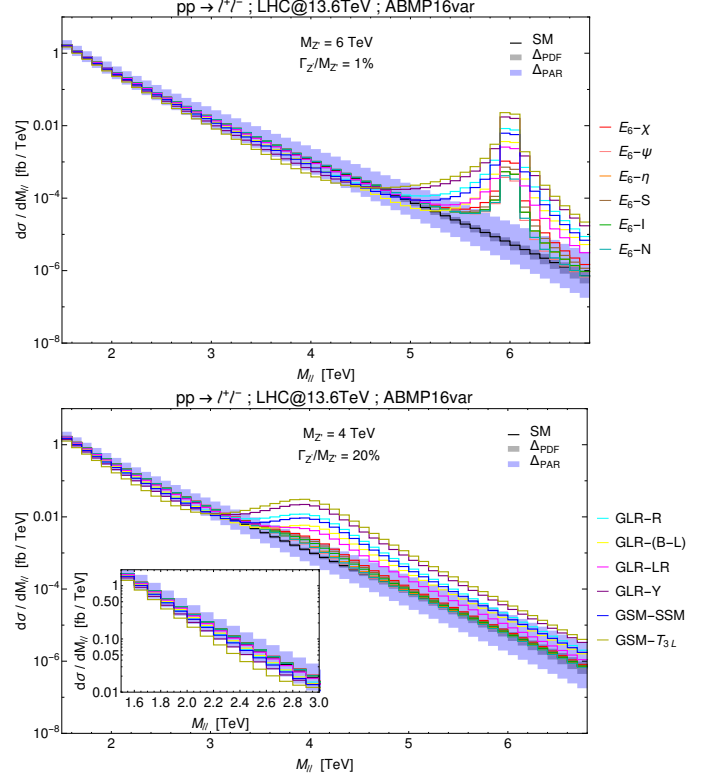


FIG. 3. Differential cross section in invariant mass of the dilepton final state at the LHC with $\sqrt{s} = 13.6$ TeV. Coloured curves are obtained for a series of single Z' benchmark models, where we set (top) $M_{Z'} = 6$ TeV, $\Gamma_{Z'}/M_{Z'} = 1\%$ and (bottom) $M_{Z'} = 4$ TeV, $\Gamma_{Z'}/M_{Z'} = 20\%$.

the NNPDF A_{FB}^* prediction in the bottom panel of Fig. 2 decreasing and turning negative around $M_{\ell\ell} \approx 5$ TeV.

In order to constrain quark distributions in the region $0.4 \lesssim x \lesssim 0.6$, fixed-target deep inelastic scattering and forward Drell-Yan production data are usually employed. For instance, in the case of the ABMP16 set [22] it is primarily the forward LHCb [42–44] and D0 [45] data which determine the quark distributions in this region, and lead to low enough sea distributions, compared to the valence distributions, that the SM prediction for A_{FB}^* stays positive. To fully assess the high-mass asymmetry SM predictions in Fig. 2, it will be relevant both a) to verify the compatibility of high-sea NNPDF-like scenarios with forward Drell-Yan production from present and upcoming measurements, and b) to estimate the impact of large- x systematic uncertainties, such as those taken into account via the ABMP16var method, on high-sea NNPDF-like scenarios. We see from Fig. 2 that, in the low-sea ABMP-like case, these large- x systematic uncertainties, although significantly larger than the “standard” PDF uncertainties, do not however endanger the A_{FB}^* positivity in the SM. On the other hand, it cannot be ruled out that, in the high-sea NNPDF-like case, such large- x sys-

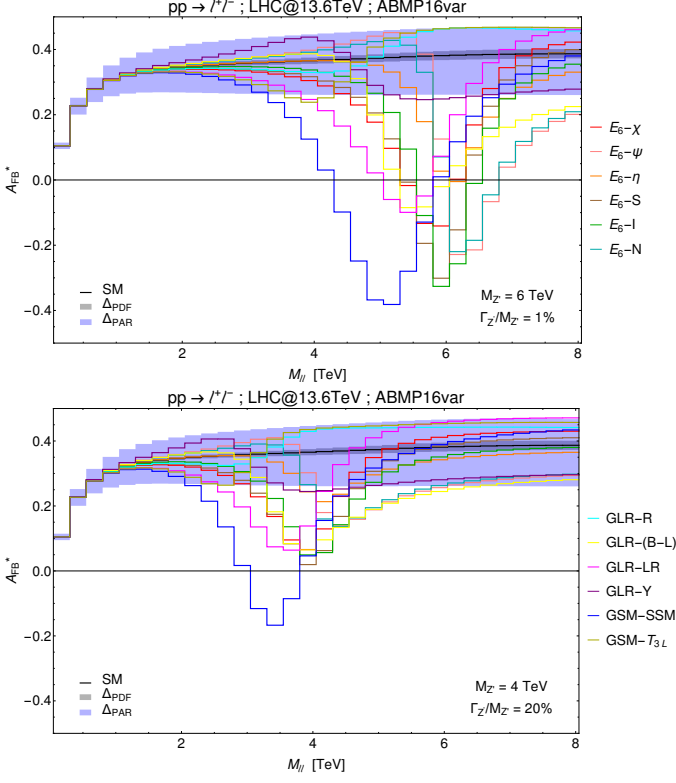


FIG. 4. Asymmetry A_{FB}^* in invariant mass of the dilepton final state at the LHC with $\sqrt{s} = 13.6$ TeV. Coloured curves are obtained for a series of single Z' benchmark models, where we set (top) $M_{Z'} = 6$ TeV, $\Gamma_{Z'}/M_{Z'} = 1\%$ and (bottom) $M_{Z'} = 4$ TeV, $\Gamma_{Z'}/M_{Z'} = 20\%$.

tematic uncertainties might yield an error band on the A_{FB}^* result in the high-mass region so large as to overcome the difference currently seen between predictions from different PDF sets. Investigations of this are warranted. This possibility underlines the relevance, even within the SM, of the studies of high- x quark density systematics proposed in the present work.

BSM searches. As the systematic uncertainty from the high- x quark density is generally comparable to or larger than the “standard” PDF error, it is important to investigate it in the context of BSM searches. In Fig. 3 we show the signal profile in the differential cross section observable for narrow (top) and wide (bottom) Z' -bosons from a series of benchmark models. They belong to Grand Unified Theory (GUT) inspired classes of models predicting a naturally heavy (narrow) Z' and have been described in [3]. While narrow resonances with masses below 5 TeV are excluded by direct searches from ATLAS [4] and CMS [5], lighter wide resonances as heavy as few TeV are still allowed, depending on their specific realisation. We set the mass of narrow Z' s ($\Gamma_{Z'}/M_{Z'} = 1\%$) at 6 TeV and of wide Z' s ($\Gamma_{Z'}/M_{Z'} = 20\%$) at 4 TeV, so as to comply with current bounds. Narrow models

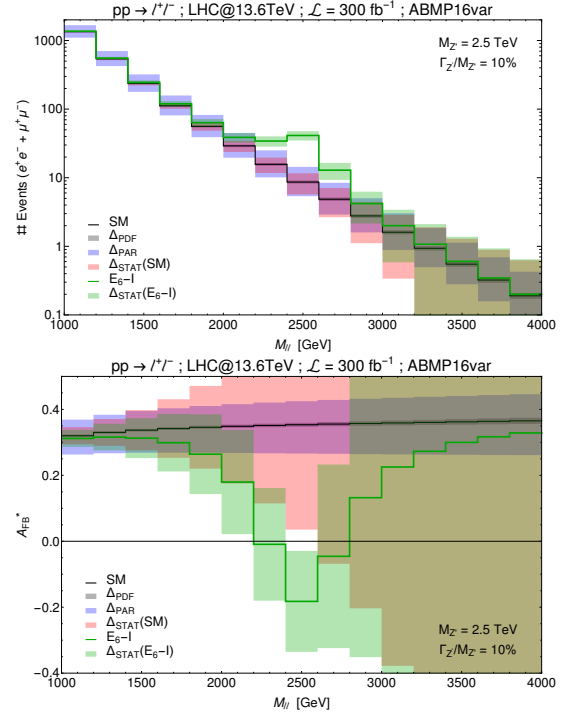


FIG. 5. Differential cross section (top) and A_{FB}^* (bottom) in invariant mass of the dilepton final state at the LHC with $\sqrt{s} = 13.6$ TeV for a Z' in the E_6 -I model, where we set $M_{Z'} = 2.5$ TeV and $\Gamma_{Z'}/M_{Z'} = 10\%$. The statistical uncertainty band corresponds to an integrated luminosity $\mathcal{L} = 300$ fb $^{-1}$, combining the statistics of the di-electron and di-muon channels.

would be marginally affected by the additional source of uncertainty, while broad resonances would potentially suffer a strong reduction of sensitivity. An interesting feature appearing more visibly in the case of wide resonances concerns the negative interference contribution occurring in the low mass tail of the distribution. The resulting depletion of events, while potentially affecting the control region in the analysis for BSM searches, can also lead to an early indication of the presence of a BSM contribution [9, 10], above and beyond SM uncertainties (for some Z' scenarios), see inset in the bottom plot.

The signal profiles in the A_{FB}^* observable of the selected benchmark models are shown in Fig. 4 for the two configurations of narrow (top) and broad (bottom) resonances. Despite the larger uncertainty band from the exponent variation method, the A_{FB}^* Z' signal shape remains well visible above the SM background predictions in both scenarios of narrow and broad resonances. The property of the A_{FB}^* of being to some extent unaffected by variations of the resonance width is a crucial feature that makes this observable a suitable discriminant in BSM searches [28].

Next, in order to assess the sensitivity of the LHC to wide Z' resonances, we perform a statistical analysis over a selected Z' benchmark model. We consider the E_6 -I

model [46] and set the Z' mass to 2.5 TeV and its width to 10% of its mass. In Fig. 5 we show the number of events (top) and the A_{FB}^* (bottom) with their statistical error in comparison with the systematic uncertainties from PDFs and from PDF parameterisation. For a realistic estimation of the statistics of such a signal, we include Next-to-Next-to-Leading Order (NNLO) QCD corrections through a K -factor computed with **DYTurbo** [47], fixing the Electro-Weak (EW) parameters to the G_μ scheme at LO. The CMS experimental acceptances and efficiencies of the di-electron and di-muon channels [5] are included and the statistics of the two final states corresponding to an integrated luminosity of 300 fb^{-1} are then combined. In this scenario, it would be possible to disentangle the BSM signal from the background in both observables. When considering only the statistical uncertainty, the significance could reach 4.4σ and 4.3σ for the bump search and for the A_{FB}^* observable, respectively. On the other hand, once systematic uncertainties are included (linearly combining the two PDF errors while summing in quadrature the statistical uncertainties) the significance is reduced to 2.9σ and 2.3σ for the cross section and A_{FB}^* observable, respectively. Therefore, in this context the significance from the A_{FB}^* still remains comparable to the cross section and, through the combination of the two, an earlier discovery can be achieved.

Conclusion and outlook. Motivated by the observation [10] that the LHC sensitivity to new gauge-boson broad resonances is significantly enhanced owing to the quark PDF improvement from the DY lepton-charge and forward-backward asymmetry analysis [15], in this paper we have studied theoretical systematic uncertainties in the multi-TeV mass region associated with the high- x quark density. Based on a remark originally made in Ref. [22], we have developed a method, which we term **ABMP16var**, to take into account the physical effects of propagating, through QCD evolution, the low-scale non-perturbative parameterisation uncertainty in the falling-off $x \rightarrow 1$ quark density to the region of the very high mass tails in dilepton distributions. We have examined the implications of this method both on SM predictions for high-mass dilepton observables and on BSM signals in a variety of narrow- Z' and wide- Z' models.

In the SM case, we find that the high- x systematic uncertainties become extremely important in the multi-TeV mass region for both the cross section $d\sigma/dM_{\ell\ell}$ and the asymmetry A_{FB}^* , outweighing the uncertainties of standard PDF sets, and thus need to be taken into account for reliable estimates of theoretical errors on SM predictions in this region. Although they are larger than standard PDF uncertainties, we find that they do not spoil the positivity and near-flatness of A_{FB}^* at high masses which characterises the results from the PDF sets **ABMP16**, **CT18** and **MSHT20**.

On the other hand, we confirm the observation [32] on

the A_{FB}^* result obtained from the PDF set **NNPDF4.0** becoming steep for $M_{\ell\ell} \gtrsim 4 \text{ TeV}$, and eventually turning negative as a consequence of the high-sea, low-valence partonic content. It remains to be seen what size uncertainties the high- x quark density systematics might give in the case of high-sea, low-valence **NNPDF**-like scenarios, and to what extent such scenarios are compatible with forward DY production measurements.

Concerning BSM signals of Z' states, we have selected benchmark models representative of the E_6 , Generalised Left-Right and Generalised Standard Model [3], taking into account that narrow resonances with masses below 5 TeV are excluded by current ATLAS and CMS bounds [4, 5], while wide resonances are still allowed below 5 TeV. Taking $M_{Z'} = 6 \text{ TeV}$, $\Gamma_{Z'}/M_{Z'} = 1\%$ for a series of narrow- Z' models and $M_{Z'} = 4 \text{ TeV}$, $\Gamma_{Z'}/M_{Z'} = 20\%$ for a series of wide- Z' models, we find that, even in the presence of systematic errors due to the high- x quark density, computed via the **ABMP16var** method, the BSM signal profiles remain visible against the SM background in the 3 - 6 TeV region of dilepton final states. This applies to both the cross section and A_{FB}^* .

We have further carried out a statistical analysis of LHC Run 3 sensitivity to wide Z' resonances, for integrated luminosity $\mathcal{L} = 300 \text{ fb}^{-1}$, using the E_6 -I model with $M_{Z'} = 2.5 \text{ TeV}$ and $\Gamma_{Z'}/M_{Z'} = 10\%$. Evaluating the reduction in the significance due to the systematic uncertainties added to the statistical ones indicates that the significance from A_{FB}^* remains comparable to that of the cross section, and that discovery can be achieved by combining the two. It is worth stressing that, going to higher invariant mass regions, one will have to deal with statistical limitations, particularly affecting A_{FB}^* , at Run 3 of the LHC. Yet, many Z' models of the above kind would still be accessible herein.

Our analysis could well be extended to the HL-LHC, affording one a tenfold increase in luminosity with respect to Run 3 of the LHC. However, in order to have a realistic estimate of the sensitivity of this LHC future configuration to the potential Z' signals considered here, one would need to make some assumptions about the final yield of the current stage of the CERN machine (i.e., either an increased limit on $M_{Z'}$ or a hypothesis of evidence or discovery for some values of it), project the PDF uncertainty following the fits to Run 3 data, and face the possibility of (recall the bottom frame of Fig. 2) entering the 5 TeV (and above) mass region, where PDF predictions for the central value of A_{FB}^* vary greatly between different sets at present, and may not have been reconciled by then. Moreover, assuming that no anomalous dilepton events will have been seen in the relevant mass region at Run 3, so that higher Z' masses than those studied here will have to be considered at the HL-LHC, it is not certain that the increase in luminosity will offset the decrease in the Z' cross section (recall Fig. 1). (Conversely, in the presence of a dilepton excess at Run 3, the

HL-LHC would obviously serve the purpose of further Z' diagnostic.) For all such reasons, we leave an HL-LHC analysis to future investigations.

Acknowledgments. The work of J. Fiaschi has been supported by STFC under the Consolidated Grant ST/T000988/1. F. Hautmann acknowledges funding from the Chinese Academy of Sciences President's International Fellowship Initiative, grant No. 2022VMA0005. S. Moretti is supported in part through the NExT Institute and acknowledges funding from the STFC Consolidated Grant ST/L000296/1. S. Moch is supported in part by the Bundesministerium für Bildung und Forschung under contract 05H21GUCCA.

* juri.fiaschi@liverpool.ac.uk

† francesco.giuli@cern.ch

‡ hautmann@thphys.ox.ac.uk

§ sven-olaf.moch@desy.de

¶ s.moretti@soton.ac.uk; stefano.moretti@physics.uu.se

- [1] P. Langacker, *Rev. Mod. Phys.* **81**, 1199 (2009), arXiv:0801.1345 [hep-ph].
- [2] E. Salvioni, G. Villadoro, and F. Zwirner, *JHEP* **11**, 068 (2009), arXiv:0909.1320 [hep-ph].
- [3] E. Accomando, A. Belyaev, L. Fedeli, S. F. King, and C. Shepherd-Themistocleous, *Phys. Rev. D* **83**, 075012 (2011), arXiv:1010.6058 [hep-ph].
- [4] G. Aad et al. (ATLAS), *Phys. Lett. B* **796**, 68 (2019), arXiv:1903.06248 [hep-ex].
- [5] A. M. Sirunyan et al. (CMS), *JHEP* **07**, 208 (2021), arXiv:2103.02708 [hep-ex].
- [6] X. Cid Vidal et al., *CERN Yellow Rep. Monogr.* **7**, 585 (2019), arXiv:1812.07831 [hep-ph].
- [7] F. Gianotti et al., *Eur. Phys. J. C* **39**, 293 (2005), arXiv:hep-ph/0204087.
- [8] T. Golling et al., arXiv:1606.00947 [hep-ph].
- [9] E. Accomando et al., *Phys. Lett. B* **803**, 135293 (2020), arXiv:1910.13759 [hep-ph].
- [10] J. Fiaschi, F. Giuli, F. Hautmann, and S. Moretti, *JHEP* **02**, 179 (2022), arXiv:2111.09698 [hep-ph].
- [11] G. Panico and A. Wulzer, *The Composite Nambu-Goldstone Higgs*, Vol. 913 (Springer, 2016) arXiv:1506.01961 [hep-ph].
- [12] G. F. Giudice, C. Grojean, A. Pomarol, and R. Rattazzi, *JHEP* **06**, 045 (2007), arXiv:hep-ph/0703164.
- [13] S. De Curtis, M. Redi, and A. Tesi, *JHEP* **04**, 042 (2012), arXiv:1110.1613 [hep-ph].
- [14] K. Agashe, R. Contino, and A. Pomarol, *Nucl. Phys. B* **719**, 165 (2005), arXiv:hep-ph/0412089.
- [15] J. Fiaschi, F. Giuli, F. Hautmann, and S. Moretti, *Nucl. Phys. B* **968**, 115444 (2021), arXiv:2103.10224 [hep-ph].
- [16] S. Alekhin et al., *Eur. Phys. J. C* **75**, 304 (2015), arXiv:1410.4412 [hep-ph].
- [17] H. Abdolmaleki et al. (xFitter) (2022) arXiv:2206.12465 [hep-ph].
- [18] E. Accomando et al., *JHEP* **10**, 176 (2019), arXiv:1907.07727 [hep-ph].
- [19] H. Abdolmaleki et al., arXiv:1907.08301 [hep-ph].
- [20] E. Accomando et al., *Eur. Phys. J. C* **78**, 663 (2018), [Erratum: *Eur. Phys. J. C* **79**, 453 (2019)], arXiv:1805.09239 [hep-ph].
- [21] E. Accomando et al., *Phys. Rev. D* **98**, 013003 (2018), [Erratum: *Phys. Rev. D* **99**, 079902 (2019)], arXiv:1712.06318.
- [22] S. Alekhin, J. Blümlein, S. Moch, and R. Placakyte, *Phys. Rev. D* **96**, 014011 (2017), arXiv:1701.05838 [hep-ph].
- [23] A. Courtoy and P. M. Nadolsky, *Phys. Rev. D* **103**, 054029 (2021), arXiv:2011.10078 [hep-ph].
- [24] R. Abdul Khalek et al. (NNPDF), *Eur. Phys. J. C* **79**, 931 (2019), arXiv:1906.10698 [hep-ph].
- [25] J. McGowan, T. Cridge, L. A. Harland-Lang, and R. S. Thorne, (2022), arXiv:2207.04739 [hep-ph].
- [26] V. Bertone, G. Bozzi, and F. Hautmann, in *29th Int. Workshop on Deep-Inelastic Scattering* (2022) arXiv:2205.15900 [hep-ph].
- [27] V. Bertone, G. Bozzi, and F. Hautmann, *Phys. Rev. D* **105**, 096003 (2022), arXiv:2202.03380 [hep-ph].
- [28] E. Accomando, A. Belyaev, J. Fiaschi, K. Mimasu, S. Moretti, and C. Shepherd-Themistocleous, *JHEP* **01**, 127 (2016), arXiv:1503.02672 [hep-ph].
- [29] T.-J. Hou et al., *Phys. Rev. D* **103**, 014013 (2021), arXiv:1912.10053 [hep-ph].
- [30] S. Bailey, T. Cridge, L. A. Harland-Lang, A. D. Martin, and R. S. Thorne, *Eur. Phys. J. C* **81**, 341 (2021), arXiv:2012.04684 [hep-ph].
- [31] R. D. Ball et al. (NNPDF), *Eur. Phys. J. C* **82**, 428 (2022), arXiv:2109.02653 [hep-ph].
- [32] R. D. Ball, A. Candido, S. Forte, F. Hekhorn, E. R. Nocera, J. Rojo, and C. Schwan, (2022), arXiv:2209.08115 [hep-ph].
- [33] S. Yang, Y. Fu, M. Liu, L. Han, T.-J. Hou, and C. P. Yuan, *Phys. Rev. D* **106**, 033001 (2022), arXiv:2202.13628 [hep-ph].
- [34] S. Yang, M. Xie, Y. Fu, Z. Zhao, M. Liu, L. Han, T.-J. Hou, and C. P. Yuan, *Phys. Rev. D* **106**, L051301 (2022), arXiv:2207.02072 [hep-ph].
- [35] M. Xie, S. Yang, Y. Fu, M. Liu, L. Han, T.-J. Hou, S. Dulat, and C. P. Yuan, (2022), arXiv:2209.13143 [hep-ex].
- [36] S. Yang, Y. Fu, M. Liu, R. Zhang, T.-J. Hou, C. Wang, H. Yin, L. Han, and C. P. Yuan, (2021), arXiv:2108.06550 [hep-ph].
- [37] Y. Fu, S. Yang, M. Liu, L. Han, T.-J. Hou, C. Schmidt, C. Wang, and C. P. Yuan, *Chin. Phys. C* **45**, 053001 (2021), arXiv:2008.03853 [hep-ex].
- [38] C. Willis, R. Brock, D. Hayden, T.-J. Hou, J. Isaacson, C. Schmidt, and C.-P. Yuan, *Phys. Rev. D* **99**, 054004 (2019), arXiv:1809.09481 [hep-ex].
- [39] E. Accomando, J. Fiaschi, F. Hautmann, S. Moretti, and C. H. Shepherd-Themistocleous, *Phys. Rev. D* **95**, 035014 (2017), arXiv:1606.06646 [hep-ph].
- [40] E. Accomando, J. Fiaschi, F. Hautmann, S. Moretti, and C. H. Shepherd-Themistocleous, *Phys. Lett. B* **770**, 1 (2017), arXiv:1612.08168 [hep-ph].
- [41] A. Bodek, J. Han, A. Khukhunaishvili, and W. Sakumoto, *Eur. Phys. J. C* **76**, 115 (2016), arXiv:1507.02470 [hep-ex].
- [42] R. Aaij et al. (LHCb), *JHEP* **01**, 155 (2016), arXiv:1511.08039 [hep-ex].
- [43] R. Aaij et al. (LHCb), *JHEP* **08**, 039 (2015), arXiv:1505.07024 [hep-ex].
- [44] R. Aaij et al. (LHCb), *JHEP* **05**, 109 (2015), arXiv:1503.00963 [hep-ex].

- [45] V. M. Abazov et al. (D0), Phys. Rev. D **91**, 032007 (2015), [Erratum: Phys.Rev.D 91, 079901 (2015)], arXiv:1412.2862 [hep-ex].
- [46] J. L. Hewett and T. G. Rizzo, Phys. Rept. **183**, 193 (1989).
- [47] S. Camarda et al., Eur. Phys. J. C **80**, 251 (2020), [Erratum: Eur.Phys.J.C 80, 440 (2020)], arXiv:1910.07049 [hep-ph].